Contactless electroreflectance study of Fermi-level pinning at the surface of cubic GaN

R. Kudrawiec,[1,a] E. Tschumak,[2] J. Misiewicz,[1] and D. J. As[2]

[1]*Institute of Physics, Wrocław University of Technology, Wybrzeże Wyspiańskiego 27, 50-370 Wrocław, Poland*
[2]*Department Physik, Universität Paderborn, Warburger Strasse 100, D-33095 Paderborn, Germany*

Van Hoof structures C. Van Hoof, K. Deneffe, J. De Boeck, D. J. Arent, and G. Borghs, [Appl. Phys. Lett. **54**, 608 (1989)] with various thicknesses of the undoped layer, for which a homogeneous built-in electric field is expected, were grown for studies of the Fermi-level pinning at the surface of cubic GaN. The built-in electric field in the undoped GaN layer was determined from contactless electroreflectance measurements of Franz–Keldysh oscillations. A good agreement between the determined and calculated electric field has been found for the Fermi-level located ~0.4 eV below the conduction band at the surface. © *2010 American Institute of Physics*. [doi:10.1063/1.3455907]

The recent progress in the growth of cubic GaN (bulk crystals and heteroepitaxial templates)[1,2] opens a way to fabricate good quality optoelectronic devices.[3–6] However, some fundamental properties of cubic GaN are still unexplored or known with a small accuracy. One of them is the Fermi-level pinning at the cubic GaN surface (i.e., the surface potential barrier), which is responsible for the formation of Schottky contact and other phenomena in semiconductor devices. Usually, the surface potential barrier is estimated from electrical measurements (e.g., I-V characteristic for metal/semiconductor interface) but the accuracy of this approach can be disputable because of its contact character (i.e., the formation of a metal contact on the semiconductor surface influences the Fermi-level position on this surface). In order to determine the Fermi-level pinning on a clear semiconductor surface, contactless methods are required.

Modulation spectroscopy [photoreflectance and contactless electroreflectance (CER)] is known as a very powerful contactless method to investigate the Fermi-level position in semiconductor structures, including the Fermi-level pinning at the semiconductor surface. So far this technique has been applied many times to investigate the energy gap of cubic GaN or the energy splitting between light and heavy holes[7–10] but this method has never been applied to study the Fermi-level pinning at the surface of cubic GaN material (i.e., the surface potential barrier in this material). This paper addresses this issue. In order to investigate the surface potential barrier in cubic GaN, we grew Van Hoof structures[11] based on cubic GaN and applied the CER to study the built-in electric field in these structures. The surface potential barrier has been determined within the approach proposed by Van Hoof,[11] which was also used recently by other authors in different material systems.[12,13]

In Fig. 1 the Van Hoof structure and the expected distribution of the electric field are shown schematically. Nominally undoped GaN cap layers of thicknesses of $d=30$, 50, 70, and 90 nm, were grown on top of 700 nm thick Si doped cubic GaN epilayers by plasma-assisted molecular beam epitaxy on free-standing 3C–SiC (001) substrates. Relevant details on the growth procedure were reported in Ref. 6. Capacity voltage (CV) measurements performed on these structures at 1 MHz showed a back ground carrier concentration of about $1-2 \times 10^{17}$ cm^{-3} for the nominally undoped cap layers and about $1-2 \times 10^{18}$ cm^{-3} for the Si doped regions.

The structural properties of GaN layers were investigated by the high resolution x-ray diffraction and atomic force microscopy. It has been concluded from these studies that the four samples have very similar structural quality [for all the samples the full width half maximum of the (002) diffraction peak equals 18 ± 1 arcmin and the root mean
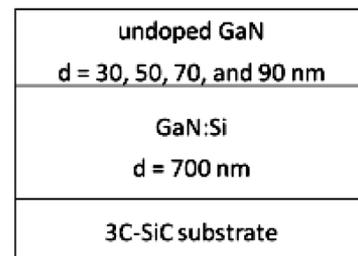
FIG. 1. (a) Schematic diagram of layers in Van Hoof structures. (b) Schematic illustration of the distribution of the built-in electric field in Van Hoof structures; the horizontal dashed line, which is indicated by E_F, corresponds to the Fermi level position.

a)Electronic mail: robert.kudrawiec@pwr.wroc.pl.
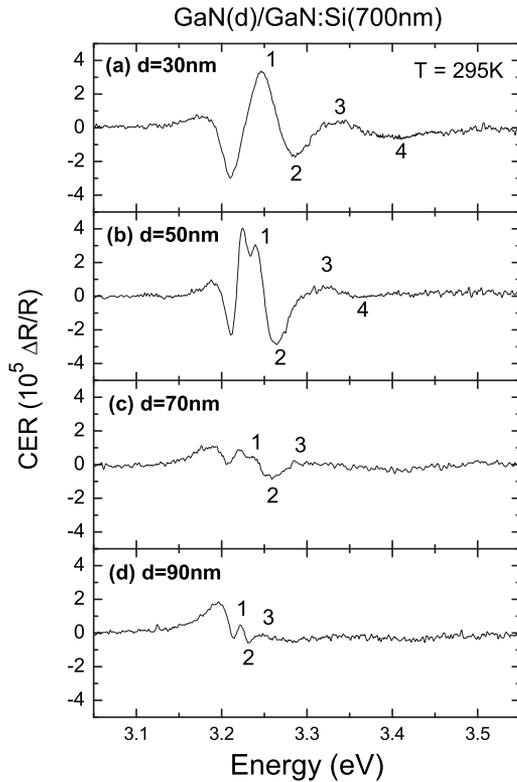
FIG. 2. Room temperature CER spectra for the cubic GaN-based Van Hoof structures with (a) 30, (b) 50, (c) 70, and (d) 90 nm thick undoped GaN layer.

square surface roughness is in the range of 5–10 nm for a 5×5 μm^2 area]. It means that the observed changes in CER spectra are associated with the variation in the electric field in these structures, which are caused by the different thickness of the undoped GaN top layer.

For CER measurements the samples were mounted in a capacitor with the top electrode made from a copper-wire mesh which is semitransparent for light. This electrode was kept at a distance of ~0.5 mm from the sample surface while the sample itself was fixed on the bottom copper electrode. A maximum peak-to-peak alternating voltage of ~3.0 kV with the frequency of 285 Hz was applied. Other relevant details of CER measurements are described in Refs. 14 and 15. For this study all CER measurements were performed in an ambient air at room temperature.

Figure 2 shows room temperature CER spectra of Van Hoof structures with various thicknesses of the undoped GaN layer. First, it is clearly visible that the CER signal changes very significantly between the four samples. Moreover, it is also observed that this signal possesses the Franz–Keldysh oscillation (FKO), which is typical for photon absorption in bulklike layers with the built-in electric field.[16] Because of the architecture of Van Hoof structures and a small depth of sample probing by CER technique,[9] the whole CER signal can be attributed to the GaN top layer, i.e., the layer with the homogeneous built-in electric field. It means that the observed change in CER signal is associated with the change in the built-in electric field in the undoped GaN layer. According to Fig. 1 a decrease in the built-in electric field is expected when the thickness of the undoped layer is increased. This decrease should be manifested by shortening of FKO period. Such an effect is clearly visible in the CER
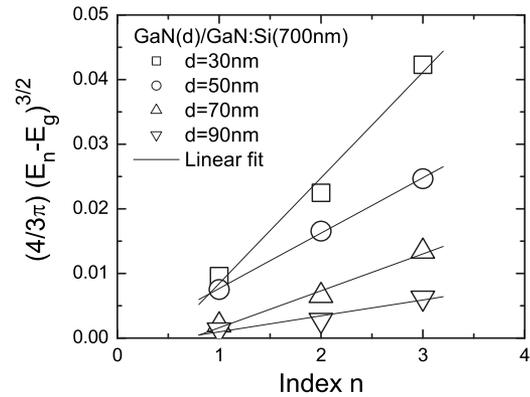
FIG. 3. Analysis of the built-in electric field in the undoped GaN layer.

spectra in Fig. 2–see the marked minima and maxima. However, it is worth noting that in general two optical transitions followed by FKO with different periods are expected in CER spectra of cubic GaN due to the strain-related splitting between heavy and light holes and due to different effective masses for heavy and light holes. But in our case the broadening of optical transitions is quite large at room temperature and therefore our spectra can be approximated by a single CER resonance followed by a single FKO.

A conventional method to determine the built-in electric field from FKO is to use an asymptotic expression for electroreflectance[17]

$$\frac{\Delta R}{R} \propto \exp\left[\frac{-2\Gamma\sqrt{E-E_g}}{(\hbar\theta)^{3/2}} \right] \cos\left[\frac{4}{3}\left(\frac{E-E_g}{\hbar\theta} \right)^{3/2} \right. $$
$$\left. + \varphi \right] \frac{1}{E^2(E-E_g)},$$
$$(\hbar\theta)^3 = \frac{e^2\hbar^2 F^2}{2\mu}, \tag{1}$$

where $\hbar\theta$ is the electro-optic energy, Γ is the linewidth, φ is an angle, F is the electric field, and μ is the electron hole reduced mass (for cubic GaN μ is assumed to be 0.11 m_0 after Ref. 18). The extrema of FKO are given by

$$n\pi = \varphi + \frac{4}{3}\left[\frac{(E_n - E_g)}{\hbar\theta} \right]^{3/2}, \tag{2}$$

where n is the index of the n-th extremum and E_n is the corresponding energy. A plot of $(E_n - E_g)^{3/2}$ versus n yields a straight line with a slope proportional to F. An analysis of the GaN-related FKO period for the five Van Hoof structures is shown in Fig. 3. Assuming that the internal electric field in GaN is homogeneous [as shown in the sketch in Fig. 1(b)] it has been determined that the built-in electric field in the undoped GaN layer equals 142 kV/cm, 75 kV/cm, 50 kV/cm, and 26 kV/cm for the Van Hoof structure with 30 nm, 50 nm, 70 nm, and 90 nm thick top layer, respectively.

For Van Hoof structures the built-in electric field in the undoped GaN layer results from the thickness of the layer and the Fermi-level pinning at GaN surface and GaN/GaN:Si interface. For the interface the Fermi-level is located at the conduction band because of Si doping. In the case of the GaN surface, the pinning of the Fermi-level is the property of a given material, its crystallographic orientation as well the surface treatment. The pinning of the Fermi-level at cubic
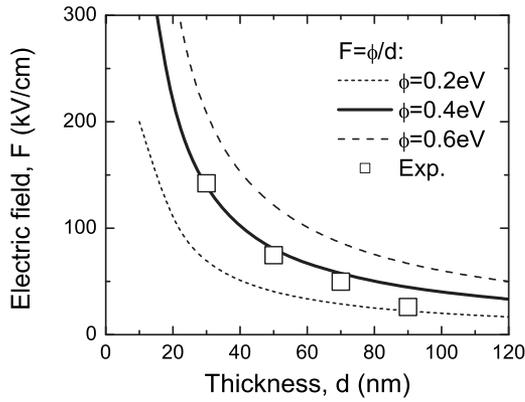
FIG. 4. Built-in electric field determined from FKO analysis (open squares) together with the fitting curve (thick solid line) and two additional curves obtained for larger (dashed line) and smaller (dotted line) parameter ϕ.

GaN surface with (001) crystallographic orientation (i.e., the surface potential barrier) is the subject of this paper. In order to determine this property, the obtained built-in electric fields have been plotted in Fig. 4 and fitted by the formula $F = \phi/d$ with the surface potential barrier ϕ treated as a free parameter. The best fit has been found for $\phi = 0.39 \pm 0.05$ eV. It is worth noting that the surface potential barrier can be determined for the each Van Hoof structure independently. For the structure with 30 nm, 50 nm, 70 nm, and 90 nm thick undoped GaN layer the ϕ potential equals 0.43 eV, 0.38 eV, 0.35 eV, and 0.23 eV, respectively. The decrease in ϕ potential with the increase in GaN layer thickness is associated with a residual background doping in this layer, which is difficult to reduce in the present technology of cubic GaN. It means that the ϕ potential determined for the set of four Van Hoof structures in Fig. 4 should be treated as an estimation of the lower boundary of the surface potential barrier. The background doping is less important for Van Hoof structures with the thinner undoped GaN layer (e.g., 30 nm) and, therefore, the ϕ potential determined for such a sample is closer to the real value of the surface potential barrier. Finally we concluded that for cubic GaN surface with the (001) crystallographic orientation the Fermi-level is pinned ~ 0.4 eV below the conduction band.

In the case of hexagonal GaN grown by plasma assisted molecular beam epitaxy, it was reported that the surface potential barrier equals 0.30 eV (but before air exposition, this barrier was 0.55 eV).[19] Recently the surface potential barrier was studied for AlGaN/GaN heterostructures capped by 3 nm thick GaN layer.[20] For samples grown by plasma assisted molecular beam epitaxy the surface potential barrier was 0.61 ± 0.10 eV. Smaller potential barrier (0.26 ± 0.04 eV) was observed for samples grown by metal-organic vapor-phase epitaxy. It means that the surface potential barrier in hexagonal GaN is very small in the comparison with its energy gap (0.26–0.61 versus 3.4 eV). The same feature is observed for cubic GaN reported in this paper (0.4 versus 3.2 eV).

In conclusion, CER spectroscopy has been applied to study the Fermi-level pinning at the surface in Van Hoof structures composed of cubic GaN. It has been clearly observed that the FKO period shortens when the thickness of the undoped GaN layer is increased. Assuming a homogeneous built-in electric field in the undoped GaN layer, it has been determined that for the cubic GaN surface with (100) orientation the Fermi-level is pinned ~ 0.4 eV below the conduction band.

[1] S. V. Novikov, N. M. Stanton, R. P. Campion, R. D. Morris, H. L. Geen, C. T. Foxon, and A. J. Kent, Semicond. Sci. Technol. **23**, 015018 (2008).
[2] J. A. Freitas, J. Phys. D **43**, 073001 (2010), and references therein.
[3] H. Yang, L. X. Zheng, J. B. Li, X. J. Wang, D. P. Xu, Y. T. Wang, X. W. Hu, and P. D. Han, Appl. Phys. Lett. **74**, 2498 (1999).
[4] D. J. As, A. Richter, J. Busch, M. Lübbers, J. Mimkes, and K. Lischka, Appl. Phys. Lett. **76**, 13 (2000).
[5] E. A. DeCuir, M. O. Manasreh, E. Tschumak, J. Schörmann, D. J. As, and K. Lischka, Appl. Phys. Lett. **92**, 201910 (2008).
[6] D. J. As, Microelectron. J. **40**, 204 (2009).
[7] G. Ramírez-Flores, H. Navarro-Contreras, A. Lastras-Martinez, R. C. Powell, and J. E. Greene, Phys. Rev. B **50**, 8433 (1994).
[8] R. Katayama, M. Kuroda, K. Onabe, and Y. Shiraki, Phys. Status Solidi C **0**, 2597 (2003)
[9] O. C. Noriega, A. Tabata, J. A. N. T. Soares, S. C. P. Rodrigues, J. R. Leite, E. Ribeiro, J. R. L. Fernandez, E. A. Meneses, F. Cardeira, D. J. As, D. Schikora, and K. Lischka, J. Cryst. Growth **252**, 208 (2003).
[10] C. Bru-Chevallier, S. Fanget, and A. Philippe, Phys. Status Solidi A **202**, 1292 (2005).
[11] C. Van Hoof, K. Deneffe, J. De Boeck, D. J. Arent, and G. Borghs, Appl. Phys. Lett. **54**, 608 (1989).
[12] H. Chouaib, C. Bru-Chevallier, A. Apostoluk, W. Rudno-Rudzinski, M. Lijadi, and P. Bove, Appl. Phys. Lett. **93**, 041913 (2008).
[13] R. Kudrawiec, H. B. Yuen, S. R. Bank, H. P. Bae, M. A. Wistey, J. S. Harris, M. Motyka, and J. Misiewicz, J. Appl. Phys. **102**, 113501 (2007).
[14] M. Motyka, R. Kudrawiec, and J. Misiewicz, Phys. Status Solidi A **204**, 354 (2007).
[15] R. Kudrawiec and J. Misiewicz, Rev. Sci. Instrum. **80**, 096103 (2009).
[16] H. Shen and M. Dutta, J. Appl. Phys. **78**, 2151 (1995), and references therein.
[17] D. E. Aspnes and A. A. Studna, Phys. Rev. B **7**, 4605 (1973).
[18] I. Vurgaftman and J. R. Meyer, J. Appl. Phys. **94**, 3675 (2003).
[19] M. Kočan, A. Rizzi, H. Luth, S. Keller, and U. K. Mishra, Phys. Status Solidi B **234**, 773 (2002).
[20] K. Köhler, S. Muller, R. Aidam, P. Waltereit, W. Pletschen, L. Kirste, H. P. Menner, W. Bronner, A. Leuther, R. Quay, M. Mikulla, O. Ambacher, R. Granzner, F. Schwierz, C. Buchhiem, and R. Goldhahn, J. Appl. Phys. **107**, 053711 (2010).